IOPscience iopscience.iop.org

Home Search Collections Journals About Contact us My IOPscience

Self-absorption and phonon-assisted radiative energy transfer processes in a ruby laser rod

This article has been downloaded from IOPscience. Please scroll down to see the full text article.

1994 J. Phys.: Condens. Matter 6 4661

(http://iopscience.iop.org/0953-8984/6/25/005)

View the table of contents for this issue, or go to the journal homepage for more

Download details:
IP Address: 171.66.16.147
The article was downloaded on 12/05/2010 at 18:40

Please note that terms and conditions apply.

J. Phys.: Condens. Matter 6 (1994) 4661–4672. Printed in the UK

Self-absorption and phonon-assisted radiative energy transfer processes in a ruby laser rod

X X Zhang†, P Hong†, B Di Bartolo‡, C W Struck§ and M Bass†‖

† Center for Research and Education in Optics and Lasers (CREOL), University of Central Florida, Orlando, FL 32826, USA

‡ Department of Physics, Boston College, Chestnut Hill, MA 02167, USA

§ Osram Sylvania, 100 Endicott Street, Danvers, MA 01923, USA

‖ Department of Electrical Engineering and Physics, University of Central Florida, Orlando, FL 32826, USA

Received 6 January 1994

Abstract. Systematic investigations of the effect of self-absorption on the dynamic and steady-state spectroscopic properties in ruby have been carried out at different temperatures (from ~ 130 to 500 K) using a long, pink laser rod. At about 140 K, the lengthening of decay times of the R lines reached a maximum and then decreased with increasing geometric trapping. Spectral diffusion as large as 10 cm^{-1} was observed in the complete-trapping regime. These observations suggest reexamination of the theoretical model for phonon-assisted radiative energy transfer in ruby.

1. Introduction

When radiation is emitted by an atom (or ion) in the transition from an excited state to a ground state, it may, after traversing a short distance through the medium, be absorbed by another atom (or ion) of the same type in the ground state, thereby raising the latter to the excited state. This phenomenon is called 'self-absorption'. Self-absorption can have both dynamic and static effects on the spectroscopic properties. It causes the lengthening of the observed decay time beyond the intrinsic radiative decay time and it leads to the self-reversal of the observed emission under certain conditions. Self-absorption is a well known phenomenon in gaseous luminescence, such as in an Hg discharge, and was theoretically addressed as early as 1922 by Compton [1] and later by others [2–5]. The major concern of these studies was the dependence of the observed decay rate on the gas density.

Self-absorption in ruby was first proposed by Varsanyi *et al* [6] as the cause of the particular intensity ratios of Zeeman components in a dilute ruby sample. It was also confirmed by many authors (see, e.g., [7]–[11]) who observed the lengthening of the decay time of the R lines in the bulk samples and by others who performed time-resolved FLN (fluroescence line narrowing) experiments [12]. The condition for the self-reversal of R lines was first given by Jekeli [13], although the phenomenon was reported as early as 1911 by Du Bois and Elias [14].

The situation is complicated by the inhomogeneous broadening of the absorption and emission lines in solids, where it is more appropriate to consider self-absorption as an energy transfer process between inhomogeneously perturbed sites whose energy mismatch can be made up by phonon energy. The energy transfer is obviously radiative in nature since the interaction between the two sites is mediated by a real photon. As a result, it is called

0953-8984/94/254661+12$19.50 © 1994 IOP Publishing Ltd

phonon-assisted radiative energy transfer. The issue of phonon-assisted radiative energy transfer has been theoretically formulated by Holstein *et al* [15, 16], who predicted that a one-site two-phonon-assisted resonant process involving the 29 cm^{-1} phonons is dominant among all possible phonon-assisted processes in ruby. This seemed to have been confirmed in time-resolved FLN experiments [12] and in the study of the 29 cm^{-1} phonon dynamics in ruby [17].

In order to discriminate non-radiative from radiative energy transfer, a dilute sample, in which no significant non-radiative energy transfer occurs, has to be used. With a long sample of this dilute material trapping can be observed, since the absorption coefficient, though small, is not negligible. However, because of the difficulties encountered in low-temperature experiments with such a long sample, no detailed experimental results have been previously reported, to the best of our knowledge, to compare to the theory. Using a home-made Dewar we have revisited this issue by carrying out a systematic study of the self-absorption effects on both steady-state and dynamic spectral properties of a ruby laser rod in the temperature range from about 130 to about 500 K. We found that the lengthening of the decay time is limited by the spectral diffusion caused by the phonon-assisted radiative energy transfer process. The one-site two-phonon-assisted resonant process does not fully account for the large spectral diffusion ($\sim$ 10 cm^{-1}) observed in this work. We present our experimental results in this paper hoping to stimulate theoretical efforts to revisit the issue of phonon-assisted radiative energy transfer.

2. Experimental results

The sample we used in this study was a ruby laser rod whose length and diamter were 16.5 and 1 cm, respectively. Both ends of the rod were polished. One of them had a Brewster angle and the other was perpendicular to the rod axis. The cylindrical surface parallel to the rod axis was ground. The ruby rod had a molar concentration of 0.05% Cr_2O_3 in Al_2O_3, which corresponds to a concentration of $N \simeq 2.4 \times 10^{19}$ Cr^{3+} ions cm^{-3}.

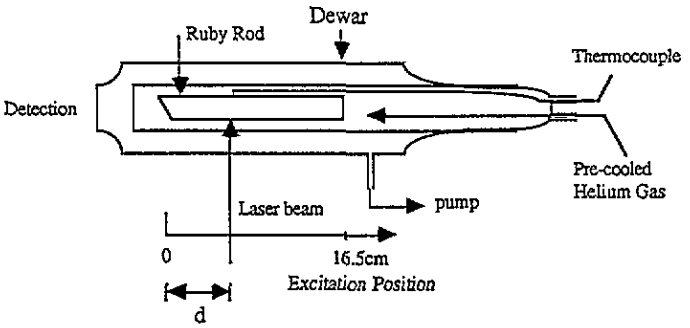

Figure 1. The schematic set-up for low-temperature experiments on the ruby rod. *d* is the distance between the centre of the detection surface and the laser spot on the rod and is referred to as the excitation position.

Because of the large size of the sample, a special Dewar was built for low-temperature experiments. He gas, precooled by liquid N_2, was brought inside the Dewar to cool down the rod (see figure 1). The lowest temperature reached was 133 K. For high-temperature

experiments the rod was placed inside a long Al pipe with a thick wall and a narrow slit (~ 1.5 mm width) through which the rod was excited. The rod could be slid along the pipe to change the excitation position. The pipe was wrapped with a heater tape and could be heated up to about 500 K.

Both steady-state luminescence spectra and radiative decays were studied. In the steady-state experiments an Omnichrome Model 532 air-cooled Ar ion laser was used as an excitation source, a Spex $\frac{3}{4}$ m grating monochromator as an analyser and an RCA 4526 (S-17) photomultiplier as a detector. The luminescence was chopped by an American Time Product mechanical chopper, which provided a reference signal for the lock-in amplifier. The signal was amplified by an EG&G 5101 lock-in amplifier and recorded on a chart recorder.

In the radiative decay experiments a Molectron DL-14 (Cooper Laser Sonics) tunable dye laser (pumped by a pulsed N_2 laser), tuned at 540 nm, was used to excite the rod. The luminescence signal was detected directly by the photomultiplier through an Oriel 52780 interference filter, which transmitted the R_1 line. The signal from the photomultiplier was amplified and processed by a Tektronix 2230 100 MHz digital storage oscilloscope, which was interfaced, through an IEEE-488 GPIB, with an IBM XT personal computer. This oscilloscope has signal-averaging capability. All the decay patterns used in this study were the average of at least 128 individual sweeps.

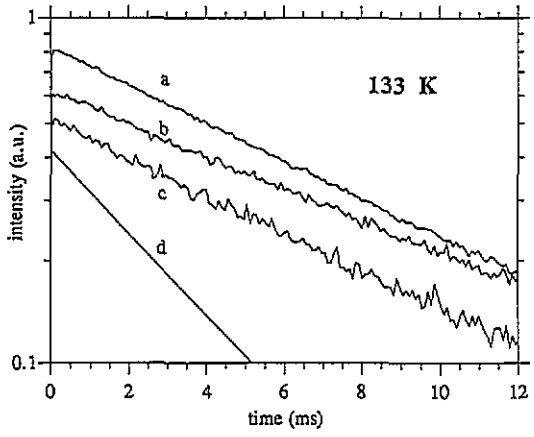

Figure 2. Decay patterns of the R_1 line of the ruby rod for different excitation positions: (a) d = 0.5 cm; (b) d = 4.5 cm; (c) d = 16.5 cm; and (d) the decay pattern with an intrinsic lifetime of 3.6 ms. d is the excitation position.

The decay patterns of the R_1 line at 133 K for different d are shown in figure 2, where d is the distance between the laser excitation spot on the rod and the detection surface of the rod (see figure 1). In what follows, d shall be referred to as the 'excitation position'. The dependences of the decay time on d for different temperatures in figure 3 show that

(i) at 133 K, the decay time increases from 8.0 to 9.32 ms, when d increases from 0.5 to about 4.5 cm, then decreases with increasing d to about 8.0 ms when d is 16.5 cm,

(ii) at 196 K, the decay time changes with the excitation position similarly to that at 133 K, but it is shorter (increasing from 5.45 to 6.55 ms then decreasing to 5.73 ms),

(iii) at room temperature (295 K), the decay time increases monotonically from 4 to about 5.1 ms,

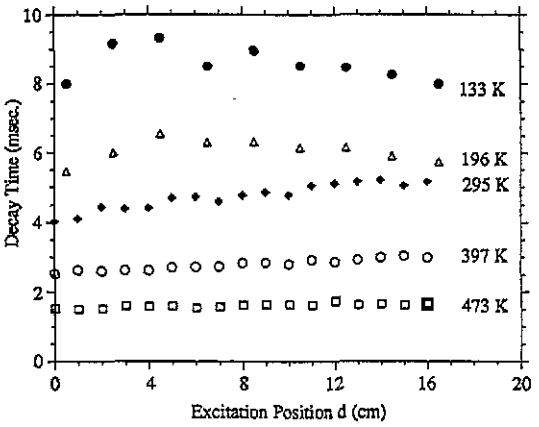

Figure 3. Observed decay times as a function of the excitation position for the ruby rod at different temperatures.

(iv) at 397 K, the decay time also increases monotonically from about 2.5 to about 3 ms, and

(v) at 473 K, the decay time is almost independent of the excitation position with a value of about 1.5 ms.

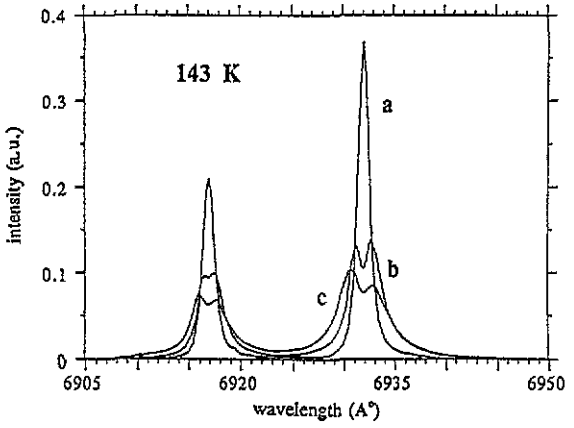

Figure 4. Normalized emission line shapes of the ruby rod for different excitation positions at 143 K: (a) $d = 0.5$ cm, (b) $d = 4.0$ cm, and (c) $d = 16.5$ cm.

The spectra at 143 and 295 K for different excitation positions are shown in figures 4 and 5 respectively. The self-reversal of the R_1 line does not happen until d increases (the excitation position is moved away from the detection end) to about 1.5 and 7 cm for $T = 143$ and 295 K respectively. The squares of the wave number difference between peaks and the valley of the self-reversed R_1 line as a function of excitation position for 143 and 295 K are given in figures 6 and 7 respectively.

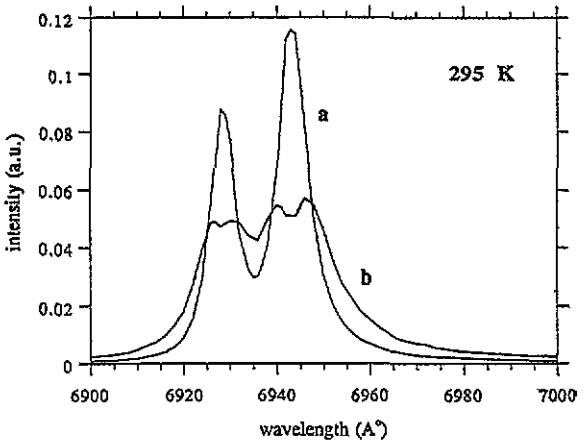

Figure 5. Normalized emission line shapes of the ruby rod for different excitation positions at 295 K: (a) $d = 0$ cm and (b) $d = 16.2$ cm.

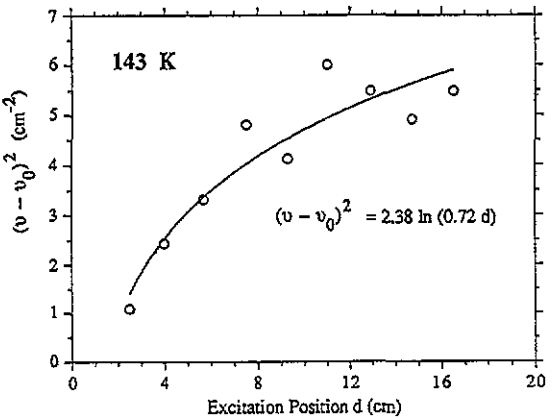

Figure 6. The square of the wave number difference between peaks and the valley of the self-reversed R_1 line as a function of the excitation position at 143 K: open circles are the experimental data and the solid line is the calculation result.

3. Discussion and interpretation of experimental results

It is well known [5] that the decay time of an emission line in the presence of self-absorption is longer than its intrinsic decay time. This is called the lengthening of the decay time. The intrinsic lifetime of ruby is 3.6 ms [18]. By comparing the observed decay patterns (figure 2(a)–(c)) to the intrinsic decay pattern (figure 2(d)) one can clearly see the lifetime lengthening due to the self-absorption. The lengthened decay patterns are essentially exponential over more than two decades. Only the first decades of the decay curves are shown in figure 2 for clarity. The exponential behaviour is present regardless of excitation position or temperature. The observed decay times at 133 K are lengthened by a factor of from 2.2 to 2.5 depending on the excitation position. This lengthening effect becomes less effective as temperature increases (see figure 3).

Assume that I_0 is the intensity of initially generated luminescence radiation. The

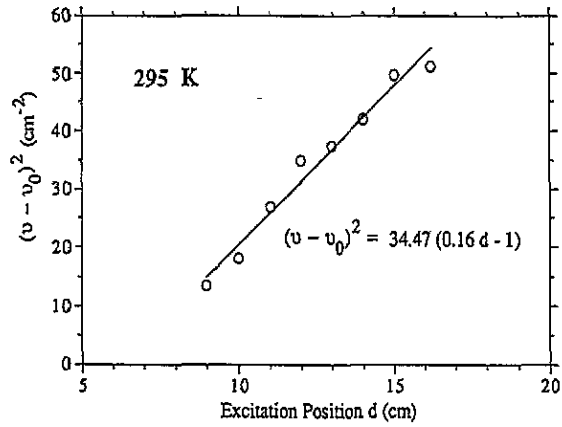

Figure 7. The square of the wave number difference between peaks and the valley of the self-reversed R_1 line as a function of the excitation position at 295 K: open circles are the experimental data and the solid line is the calculation result.

radiation penetrates an absorption layer with length d, where self-absorption occurs followed by reemission of luminescent light. If the reemitted luminescence radiation is assumed to contribute negligibly to the transmitted intensity one can write for the latter as a function of the wave number

$$I_{\text{trans}}(\nu) = I_0(\nu)\exp(-\alpha(\nu)d) \tag{1}$$

where $\alpha(\nu)$ is the absorption coefficient. Since there is no Stokes shift between the absorption and the emission of the R lines in ruby [7] the original emission peak will be more strongly absorbed and may become an intensity minimum in the transmitted spectrum, in which case the spectral line 'splits' into two peaks symmetrical about the original peak position and 'self-reversal' occurs. In order to find the position of the split peaks, one has to determine the extrema of I_{trans}, with the length of the absorption layer, d, as a parameter.

For a Gaussian or a Lorentzian line shape, assuming the line shape and the line width are the same for the emission and the absorption, the position of the split peaks, ν, can be expressed, respectively, as [13]

$$\nu - \nu_0 = \pm(\gamma/2\sqrt{\ln 2})[\ln(\alpha_{\max}d)]^{1/2} \qquad \text{for a Gaussian line} \tag{2}$$

and

$$\nu - \nu_0 = \pm(\gamma/2)(\alpha_{\max}d - 1)^{1/2} \qquad \text{for a Lorentzian line} \tag{3}$$

where ν_0 is the position of the minimum (valley) of the transmitted spectrum, γ is the spectral width of the absorption and the intrinsic emission line, and $\alpha_{\max}$ is the peak absorption coefficient. Self-reversal occurs, therefore, only for [13]

$$\alpha_{\max}d > 1. \tag{4}$$

It is interesting to note that for both Lorentzian and Gaussian line shapes the condition for the self-reversal is the same, but $(\nu - \nu_0)^2$ is a linear function of d in the former case and

is proportional to the logarithm of d in the latter case. This difference may be used to discriminate between a Lorentzian and a Gaussian line shape.

The dependence of $(\nu - \nu_0)^2$ of the self-reversed R_1 line on d was calculated using (2) and (3) for $T = 143$ and 295 K, respectively, with γ and α_{max} as adjustable parameters. The results are shown in figures 6 and 7, respectively. It can be seen from figure 7 that for $T = 295$ K the data agree very well with (3), indicating that the shape of the R_1 line at this temperature is basically Lorentzian. It can also be seen from figure 6 that for $T = 143$ K the data agree fairly well with (2), indicating that the shape of the R_1 line at this temperature has a Gaussian component, although it is not pure Gaussian. These conclusions are consistent with previous results [7]. The parameters used in the calculations are given in table 1.

Table 1. Calculation parameters for the self-reversed R_1 line.

Temperature (K)	Calculation equation	Calculation parameters (cm^{-1}) γ	α_{max}	γ (cm^{-1}) measured at $d = 0.5$ cm	α_{max} (cm^{-1}) from (4)
143	(2)	2.57	0.72	2.91	0.67
295	(3)	11.74	0.16	14.93	0.14

The calculations give $\alpha_{max} = 0.72$ and 0.16 cm^{-1} for $T = 143$ and 295 K, respectively. These values are consistent with the values, 0.67 and 0.14 cm^{-1}, obtained from (4) based on the d values at the occurrence of self-reversal. Jekeli [13] measured the absorption coefficient of the R_1 line and found that $\alpha_{max} = 3.22$ cm^{-1} at room temperature for a ruby with a concentration 20 times as high as that of the sample used in this study. Taking into account the concentration difference the agreement between the present result and the experimental data reported by Jekeli [13] is remarkable. There are no direct low-temperature absorption data available to compare the present result but it is certain that α_{max} is larger at lower temperatures although the integrated absorption coefficient of the R_1 line is almost independent of temperature [7, 13] as indicated by the present result. The larger the value of α_{max}, the shorter the average distance a photon travels through the medium before being absorbed. Therefore self-absorption is more effective at lower temperature. This can be seen from the lengthening of the decay time at different temperatures (figure 3).

Analysis of the data using (2) and (3) also gives the intrinsic spectral widths of 2.57 and 11.74 cm^{-1} for the R_1 line at $T = 143$ and 295 K respectively. The actually measured width of the unreversed R_1 line (when excited at $d = 0.5$ cm) is 2.91 cm^{-1} and 14.93 cm^{-1} for $T = 143$ and 295 K, respectively. This indicates that the emission spectrum is indeed affected by the self-absorption process even when the rod is excited at the detection end ($d \simeq 0$).

The simple considerations discussed above can indeed give one a qualitative understanding of the experimental results. However, the following more quantitative questions arise.

(i) Why does the decay time decrease for $d > 5$ cm at 133 K (figure 3)? Photons emitted at some larger d are more likely to be reabsorbed and reemitted before they eventually reach the detector. One would therefore expect the observed decay time to increase monotonically with increasing d.

(ii) Why are the two peaks of the split line not symmetric with respect to the original one? In particular, why is the higher-energy side stronger than the other side for large d ($d > 8$ cm) and the opposite for small d (figure 4)? Since there is no Stokes shift between

the absorption and the emission of the R lines in ruby [7] the split peaks in the self-reversed spectrum are expected to by symmetric with respect to the minimum. Also, why is the observed emission line for large d much broader than that for small d (in figure 8, compare curve c to curve d)?

(iii) Why, at $d \simeq 0.5$ cm, is not at least half the observed radiation seen with a decay time equal to the intrinsic radiative lifetime (3.6 ms [18])?

The key to questions (i) and (ii) lies in understanding the phonon-assisted radiative energy transfer involved in the self-absorption process. The discussion of self-reversal given above was based on the assumption that the observed photons are only the transmitted ones (i.e. once the photon is absorbed it will not be reemitted and contribute to the detected signal again). However, this assumption is not true because it has been shown by the time-resolved FLN experiments [12] that the absorbed photon not only can be reemitted but also can be reemitted with energy different from the original one due to phonon-assisted radiative energy transfer [15, 16]. When a photon is emitted at site 1 and absorbed at site 2, the excitation energy is transferred from site 1 to site 2. The transfer can be spectrally diffusive or not. If not, then a particular type of ion transfers to a like ion; if so, then the transfer is to a (slightly) dissimilar ion and requires the involvement of phonons.

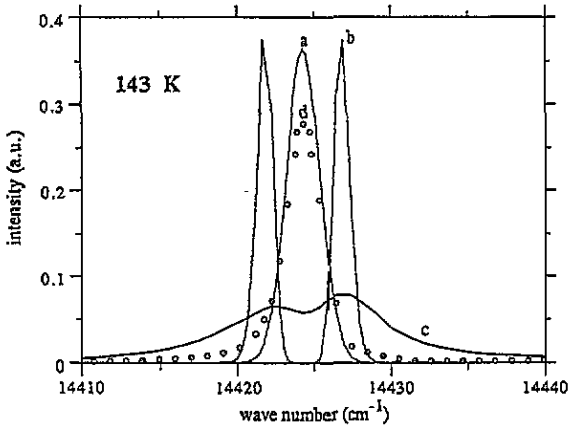

Figure 8. Normalized line shapes of the R_1 line: (a) calculated intrinsic; (b) calculated transmission from $d = 16.5$ cm; (c) observed for $d = 16.5$ cmn; and (d) observed for $d = 0.5$ cm.

The spectral diffusion can also be seen from the steady-state spectrum in figure 8. From the previous discussion we known that the intrinsic emission line shape at 143 K is approximately Gaussian, and given by [19]

$$I_0(\nu) = I_{\max} \exp(-(2\sqrt{\ln 2}/\gamma)^2(\nu - \nu_0)^2) \tag{5}$$

where γ is the spectral width of the intrinsic emission line. With the previous calculation result, $\gamma = 2.57$ cm^{-1}, the emission line shape at 143 K is plotted in figure 8, curve a. The expected transmission spectrum can be plotted, according to (1), and is given in figure 8, curve b, using the previous calculation parameter, $\alpha_{\max} = 0.72$ cm^{-1}, and the Gaussian absorption line shape [19]

$$\alpha(\nu) = \alpha_{\max} \exp(-(2\sqrt{\ln 2}/\gamma)^2(\nu - \nu_0)^2). \tag{6}$$

The actual observed R_1 line spectrum at 143 K (when the rod was excited at $d = 16.5$ cm) is also given in figure 8, curve c, for comparison. The areas of all spectra are normalized to unity.

By comparing figure 8, curve c, to figure 8, curve b, one can see, in this particular case, that more than 70% of the observed photons originate from the wings, which are spectrally diffused up to 10 cm^{-1} from the centre. This can only happen through a phonon-assisted radiative energy transfer process which alters the spectrum. We have noticed that the percentage of emission from the wings increases with increasing d. This indicates that the efficiency of the phonon-assisted radiative energy transfer process increases with increasing d.

The efficiency of the phonon-assisted radiative energy transfer process depends on the degree of radiative trapping in the sample [16], which is determined by the ratio of the geometric size of the sample to the photon mean free path. The phonon-assisted radiative energy transfer process can be 100% efficient under conditions of complete trapping, where every photon emitted is subsequently reabsorbed and reemitted until it couples with a phonon at a particular site and the energy transfer takes place. On the other hand, the photon mean free path is a strong function of the photon energy. Strong trapping may hold at the centre of the emission line but photons corresponding to the excitation energies of sites in the wings of the line will be considerably less strongly trapped.

When d reaches a value such that the phonon-assisted energy transfer process is 100% efficient, every time an emission–absorption–reemission takes place the emission is spectrally diffused from the line centre to the line wing, where the photon has a much longer free mean path and will experience less self-absorption. When d is further increased, more and more photons will be transferred from the centre to the wings so the overall trapping becomes less and less effective with increasing d, so does the lengthening of the decay time. Therefore, the decrease of the decay time with increasing d for $d > 5$ cm at 133 K (see question (i)) can be understood as the result of competition between the spectral diffusion resulting from the phonon-assisted energy transfer and the increase in geometric size. The increase in the geometric size increases the degree of radiation trapping, which in turn favours phonon-assisted energy transfer, but phonon-assisted energy transfer decreases the degree of radiation trapping due to spectral diffusion.

The second question posed earlier is, we believe, related to the specific mechanism of the phonon-assissted process, since a particular mechanism is expected to have particular effects on the emission spectrum.

Phonons can be involved in the energy transfer process in various ways, and make up the energy mismatch between sites 1 and 2. One phonon or two phonons can be involved in the process, which is then called a 'one-phonon-assisted' or a 'two-phonon-assisted' radiative energy transfer process [15, 16], respectively.

The one-phonon-assisted process is pictured in figure 9(a). A phonon is emitted or absorbed (for $\Delta E_{12} > 0$ or $\Delta E_{12} < 0$, respectively) at site 1 first followed by the emission of a photon at the same site. Then the same photon is absorbed at site 2. The energy-conserving delta function in the Fermi golden rule requires that the phonon energy be equal to the energy mismatch between the two sites. The phonon emission or absorption can also of course occur at site 2 where the photon is absorbed.

There are, in general, two types of two-phonon-assisted radiative energy transfer process depending on where the two phonons are involved. They are the so-called two-site two-phonon-assisted (TSTPA) and one-site two-phonon-assisted (OSTPA) processes, as pictured in figure 9(b) and (c) respectively. The phonon emission and the phonon absorption take place at two different sites for the TSTPA process and at the same site for the OSTPA process.

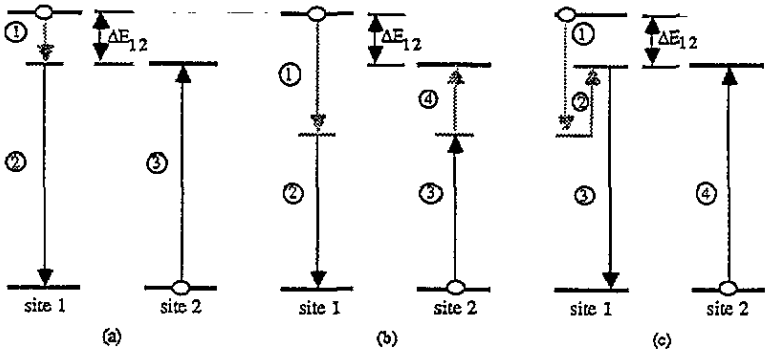

Figure 9. (a) One-phonon-assisted, (b) two-site two-phonon-assisted, and (c) one-site two-phonon-assisted radiative energy transfer processes. The solid vertical lines represent photons, the broken lines phonons, and the horizontal broken lines the intermediate states. The circled numbers represent the sequence of the perturbation chain. The open circles denote initial electronic occupancies. Downward and upward arrows represent the emission and the absorption, respectively, of photons or phonons.

The energy difference between the two phonons is equal to the electronic energy mismatch between the two sites for both cases. For the two-site process the energy of the mediating photon is equal to the electronic energy of site 1 minus (plus) the energy of the phonon emitted (absorbed) at the same site. This photon energy is usually not the same as the electronic energy of site 2 as is the case in the one-site process.

Holstein *et al* [15, 16] have theoretically studied and compared in detail the transfer rates for various phonon-assisted processes. They concluded that the one-phonon-assisted processes are much less efficient than the two-phonon-assisted ones for ruby due to the small phonon energy density of states for small energy mismatch. They also concluded that of all the possible two-phonon-assisted processes the OSTPA processes are more efficient than the TSTPA processes. In particular, they concluded that the OSTPA resonant process, which involves two resonant phonons (ones whose energies are in resonance with the energy difference between $2\bar{A}$ and $\bar{E}$ levels), is the most efficient in ruby. This idea appeared to have been confirmed by the time-resolved FLN experiment [12] and was successful in explaining the trapping of 29 cm^{-1} resonant phonons in ruby [17]. However it cannot qualitatively account for the large observed spectral diffusion ($\sim$ 10 cm^{-1}) shown in figure 8, curve c. In contrast an OSTPA resonant process can only cause a spectral diffusion up to the order of the resonance width of the 29 cm^{-1} phonons. This width is only 0.02 cm^{-1} [20]. It is possible that a TSTPA non-resonant process can qualitatively account for our observations because it involves photons whose energy is shifted by the energy of phonons from the electronic energy. Since non-resonant phonons are involved, the energy of these photons can be shifted out of the inhomogeneous broadening line width. Therefore these photons may have trapping lengths considerably in excess of the zero-phonon emission photons and may escape from the sample in the strong-trapping regime. This may account for the large observed spectral width in figure 8, curve c. As pointed out in [16], except for the previously reported results on ruby and Cr^{3+}:$LaAlO_3$, all other studies appear to exhibit TSTPA non-resonant transfer. We therefore suggest that modelling of the phonon-assisted radiative energy transfer process in ruby be revisited to identify the source of discrepancy.

Question (iii) is, we think, more profound than it seems. When the rod is excited at $d = 0.5$ cm, it is expected, according to Beer's law (using the previous result, $\alpha_{max} = 0.72$ cm^{-1}), that at least 70% of the initially generated luminescent photons will

escape the sample with the intrinsic decay time (3.6 ms) without being absorbed and contribute to the detected signal. Therefore the detected decay curve is expected to be non-exponential with the initial part having a decay time of 3.6 ms, but this component is not seen in the decay pattern (figure 2(a)): instead a pure exponential decay is seen with a single, lengthened decay time (8 ms). This implies that all the photons initially generated are completely trapped within a distance of 0.5 cm and experience the emission–absorption–reemission cycle at least twice before they escape the rod.

This is obviously inconsistent with Beer's law, which predicts that a photon will experience absorption–reemission less than once on average when the rod is excited at $d = 0.5$ cm. One of the pictures one might think about to reconcile this contradition is the migration of the excitation energy (i.e. the excitation energy migrates inward along the rod so effectively that the emission appears to come from some large d even though the rod is excited at $d = 0.5$ cm), but earlier four-wave mixing grating experiments [21–23] have shown that the energy migration in ruby is not effective and the excitation diffusion length is less than 60 nm. We therefore believe that the trapping even at small d is due to some other microscopic processes, since the same phenomenon has also been observed for a thin ($\sim$ 1 mm thickness) sample even when excited on the surface.

4. Conclusions

In conclusion, the effects of a phonon-assisted radiative energy transfer process on both the steady-state spectrum and the lengthening of the decay time have been directly observed in a long, dilute ruby rod. The saturation and reduction of the lengthening of the decay time in the complete-trapping regime was explained as a result of the spectral diffusion caused by the phonon-assisted radiative energy transfer process. Large spectral diffusion and asymmetric, self-reversed line shapes were observed at about 140 K. These results call for a reexamination of the theoretical models used to explain energy transfer in ruby. For example, there may be a geometric dependence of the radiative phonon-assisted energy transfer mechanism that must be invoked to explain our results since a long rod was used in our experiments assuring complete trapping. The data presented mean that the microscopic radiaton trapping mechanism applicable to ruby needs further study.

References

[1] Compton K T 1922 *Phys. Rev.* **20** 283
[2] Milne E A 1926 *J. London Math. Soc.* **1** 1
[3] Kenty C 1932 *Phys. Rev.* **42** 823
[4] Holstein T 1947 *Phys. Rev.* **72** 1212
[5] Holstein T 1951 *Phys. Rev.* **83** 1159
[6] Varsanyi F, Wood D L and Schawlow A L 1959 *Phys. Rev. Lett.* **3** 544
[7] Nelson D F and Sturge M D 1965 *Phys. Rev.* **7** A1117
[8] Imbusch G F 1967 *Phys. Rev.* B **153** 326
[9] Murphy J C, Aadmodt L C and Jen C K 1974 *Phys. Rev.* B **9** 2009
[10] Koo J, Walker L R and Geschwind S 1975 *Phys. Rev. Lett.* **35** 1669
[11] Birnbaum M, Fincher C L, Machan J and Bass M 1987 *AIP Conf. Proc.* vol 160 (New York: American Institute of Physics) p 240
[12] Selzer P M and Yen W M 1977 *Opt. Lett.* **1** 90
[13] Jekeli W 1965 *J. Opt. Soc. Am.* **55** 1442
[14] Du Bois H and Elias G J 1911 *Ann. Phys. Lpz.* **35** 617
[15] Holstein T, Lyo S K and Orbach R 1977 *Phys. Rev.* B **16** 934

[16] Holstein T, Lyo S K and Orbach R 1986 *Laser Spectroscopy of Solids* 2nd edn, ed W M Yen and P M Selzer (New York: Springer) p 63
[17] Meltzer R S, Rives J E and Egbert W C 1982 *Phys. Rev.* B **25** 3026
[18] Selzer P M, Huber D L, Barnett B B and Yen W M 1978 *Phys. Rev.* B **17** 4979
[19] Mitchell A C G and Zemansky M W 1961 *Resonance Radiation and Excited Atoms* (Cambridge: Cambridge University Press) ch III
[20] Sox D, Majetich S, Rives J E and Meltzer R S 1985 *J. Physique. Coll.* **46** C7 493
[21] Eichler H J, Eichler J, Knof J and Noak Ch 1979 *Phys. Status Solidi* b **52** 481
[22] Liao P F, Humphrey L M, Bloom D M and Geschwind S 1979 *Phys. Rev.* B **20** 4145
[23] Hamilton D S, Heiman D, Feinberg J and Hellwarth R W 1979 *Opt. Lett.* **4** 124